



Inter laminar failure behavior in laminate carbon nanotubes-based polymer composites

Mostapha Tarfaoui, Khalid Lafdi, Omar Hashim Hassoon, Mourad Nachtane, Ahmed El Moumen

► To cite this version:

Mostapha Tarfaoui, Khalid Lafdi, Omar Hashim Hassoon, Mourad Nachtane, Ahmed El Moumen. Inter laminar failure behavior in laminate carbon nanotubes-based polymer composites. Journal of Composite Materials, 2018, 52 (26), pp.3655-3667. 10.1177/0021998318767493 . hal-01864893

HAL Id: hal-01864893

<https://ensta-bretagne.hal.science/hal-01864893>

Submitted on 10 Feb 2023

HAL is a multi-disciplinary open access archive for the deposit and dissemination of scientific research documents, whether they are published or not. The documents may come from teaching and research institutions in France or abroad, or from public or private research centers.

L'archive ouverte pluridisciplinaire **HAL**, est destinée au dépôt et à la diffusion de documents scientifiques de niveau recherche, publiés ou non, émanant des établissements d'enseignement et de recherche français ou étrangers, des laboratoires publics ou privés.

Inter laminar failure behavior in laminate carbon nanotubes-based polymer composites

M Tarfaoui¹, A El Moumen¹ , K Lafdi², OH Hassoon¹ and M Nachtane¹

Abstract

Delamination progressive in carbon nanotubes reinforced composites under applied Short Beam Shear test was studied. Experimental characterization was carried out using ASTM D2344 standard norms for different carbon nanotubes mass fractions ranging from 0 to 4%. Failure modes and the delamination were experimentally characterized by scanning electron microscopy and Kayence microscopy to assess the failure behavior. The numerical model was created under ABAQUS software based on the cohesive zone models. The numerical model was formulated according to the damage mechanics. In these models, the cohesive interaction was implanted between elements of each fabric ply to control the initiation and the propagation of the delamination for different carbon nanotubes fractions. The force–displacement curves vs. carbon nanotubes added were obtained for the numerical model and shown to be in good agreement with the experimental data. The effect of carbon nanotubes on the progressive delamination was elucidated.

Keywords

Carbon nanotubes, laminate composites, delamination, damage, cohesive interface modeling, finite element analysis

Introduction

Laminate composites containing carbon nanotubes (CNTs) offer excellent properties to fracture and the impact strength. Inter laminar damage, also called delamination, is one of the most forms of the failure observed in these composite systems. Predicting the delamination is complicated and based on the microscopic observation or with little use numerical simulations.¹ It is divided into delamination initiation and delamination propagation.²

Some experimental investigations into damage mechanisms and the delamination were analyzed using optical and scanning electron microscopy (SEM) techniques.³ Location of inter and intra-ply damage mechanisms was experimentally identified with the help of the tomography analysis.⁴ All tomography images illustrate that the delamination transverse ply fracture is the most observed modes.⁴ Arbaoui et al.⁵ investigated experimentally the mechanical properties and the damage evolution in Glass/Vinylester laminate composites under compressive loading. They observed that the intra and inter delamination were the

most damage modes experimentally observed using imaging tools technique.

Analysis of specimens was not able to totally elucidate the delamination and the damage evolution into components of composites. An alternative technique to evaluate the delamination during mechanical tests is the use of numerical simulations. Modeling strategies for the simulating of the delamination in laminate composites was proposed in literature^{6,7} for composites aircraft structures. Jacques et al.⁸ investigated a numerical simulation approach of the delamination growth in unidirectional and textile composites using cohesive zone method. This method was also introduced by Kumar et al.⁹ in order to simulate the delamination in the carbon fiber and glass fiber reinforced polymer matrix. The authors consider laminates with various stacking

¹ENSTA Bretagne, IRDL – UMR CNRS 6027, F-29200 Brest, France

²Nanomaterials Laboratory, University of Dayton, Dayton, OH, USA

Corresponding author:

A El Moumen, ENSTA Bretagne, 2 rue François Verny, 29806 Brest Cedex 09 Brest, 29200, France.

Email: ahmed.el_moumen@ensta-bretagne.fr

sequences. The obtained results were found to be in good agreement with the experimental results. Progressive delamination simulation in composites was also proposed for Glass/Epoxy based laminate composite materials.¹⁰ The authors have shown that the finite element simulations can accurately represent the physical mechanisms controlling the damage initiation, development and the evolution and reproduce a number of the phenomena including delamination and failure. Yousefi et al.¹¹ developed a numerical model based on the interface cohesive elements to simulate the matrix cracking. They assumed equally spaced cracks based on experimental observations and measurements. Tarfaoui et al.¹² used quadratic cohesive elements to model the crack initiation and the propagation throughout composite panels. Another technique for delamination modeling using shell elements and a cohesive zone model (CZM) was proposed by Riccio and Gigliotti¹³ in order to simulate DCB, ENF and MMB experiments. A general review and detailed techniques for simulation approaches of delamination and damage in the context of the finite element method (FEM) was presented and detailed in Coelho.¹⁰

To our knowledge, little results are available in the open literature on the modeling of delamination in laminate composites reinforced with a random distribution of CNTs and subjected to the shear test. In this paper, a three dimensional FE model was developed to further understand the local damage and the delamination reproduce during Short Beam Shear Test (SBST) on laminate composites reinforced with CNTs. Experimental studies and microscopic observations were carried. Based on these imaging characterizations, the delamination zones were identified and with the help of these observations, the placement of cohesive zone elements can be implemented into the model. Finally, progressive damage model is created by applying failure criteria and the damage degradation model in the ABAQUS software.

Material, process, and experimental characterization

Morphologies and manufacturing process

In this study, composite specimens consist of nanocomposite film made of Epoxy resin reinforced with added CNTs. The fabricated film is placed between plies of laminate carbon fibers fabric. Five specimens with CNTs fraction of 0%, 0.5%, 1%, 2%, and 4% were manufactured and experimentally tested under SBST. First, CNTs were mixed with Epoxy resin, for 30 min, using a high shear laboratory mixer at 2000 r/min and then the ultrasonic path was used to obtain a homogeneous mixture and to guarantee a better dispersion of nanotubes into matrix. The film with 120 μm in thickness containing CNTs is then obtained using film line. Once the film is made, we make laminates with the film as interleave between carbon fabrics and cured in the hot press. All panels, with 12 layers of carbon fibers interleaved by 11 layers of CNTs film, were manufactured using infusion process under a pressure of 200 MPa. Figure 1 shows the morphology of CNTs and their distribution into epoxy at different magnifications using SEM. It appears that the nanotubes have the tube-shaped materials form and considered as a long curved cylindrical fibers as snake-like shapes. These nanotubes have a tendency to cluster and to create some aggregates with agglomerations.

Experimental characterization

Composite specimens consist of 12 plies with 4 mm of the total thickness. SBST Experimental characterization was conducted with ASTM D 2344 standard norms. Figure 2 illustrates the experimental test and the dimensions of the panels. As the ASTM D 2344 standard prescribes, a specimens with $L=26\text{ mm}$, $W=8\text{ mm}$, and $T=4.1\text{ mm}$ has been used. For each CNTs fraction, the test is repeated 10 times in order to assure the reproducibility of experimental results.

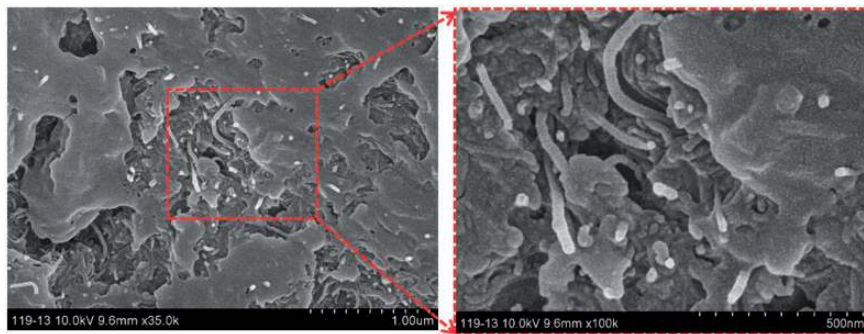


Figure 1. Distribution of nanotubes in epoxy resin creating the aggregates.

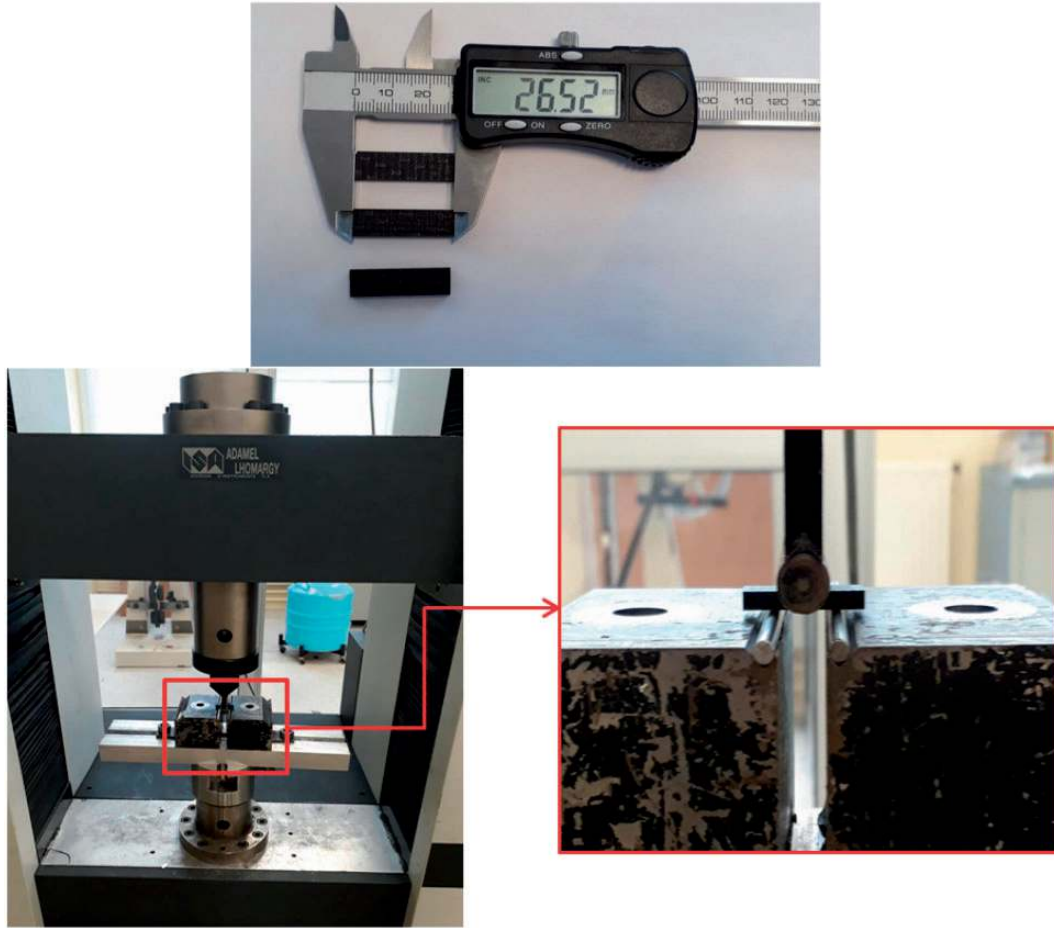


Figure 2. Dimension of the specimen (in mm) and the experimental shear test rig.

Figure 3 shows the force–displacement curves vs. CNTs fraction. The curves were very reproducible for all different CNTs percentage. The average curve is also plotted and presented in Figure 3(f). The general tendency is that the force level is increased by the addition of CNTs which indicates the role of CNTs as reinforcement. However a drop was recorded in the case of 4% of CNTs. At higher CNTs > 4%, the CNT tends to agglomerate and behave like an inclusion defect. These experimental results were used to validate finite element models with delamination.

The average value of maximum load and stiffness vs CNTs fractions were calculated and plotted in Figure 4. Adding of a small fraction of CNTs less than 2% seems to improve the mechanical properties of laminate composites. However, at 4% of CNTs there is a considerable drop of properties. The maximum load and stiffness of 0% of CNTs are respectively 1.71 kN and 5.37 kN/mm, while with 1% of CNTs its increase to 1.91 kN and 5.65 kN/mm, respectively. Therefore a gain of 10% was obtained. Moreover, it appears an important drop and degradation in properties for 4%

of CNTs, from 1.91 kN (with 1% of CNTs) to 1.04 kN (with 4% of CNTs). This degradation most likely caused by the agglomeration of nanotubes in the case of 4%-CNTs, which play the role of the defect, Figure 5.

Observation of the delamination with light microscope

Damage in laminated composites such as cracking of constituents and the delamination were not totally visible, mostly when the total fracture of specimens is not complete. To understand it, microscopy characterization was carried out. The observed microstructures of fractured specimens under SBST are shown in Figure 6. These images demonstrate inter and intra-ply failure and cracking of constituents. Various damages appear in the form of axial cracks and the delamination opens up and propagates along the same interface or changes to other interfaces creating multiple delaminations. The most obvious delamination was between ply-4 and ply-8, while the other damages are distributed at the middle region and ends zones of the specimen.

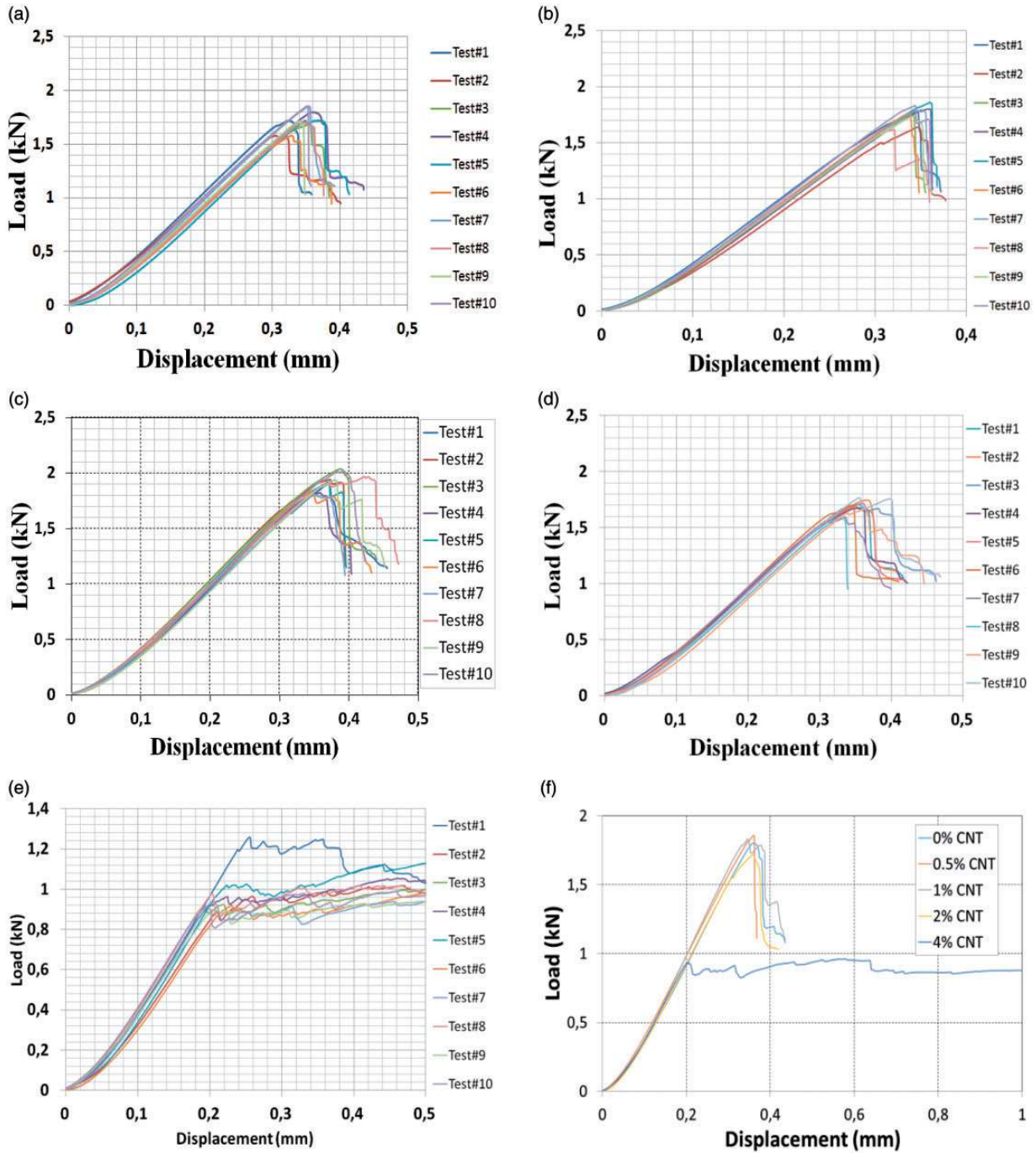


Figure 3. Typical load–displacement curves showing reproducibility of tests and average variation vs. fraction of CNTs. (a) 0% of CNTs, (b) 0.5% of CNTs, (c) 1% of CNTs, (d) 2% of CNTs, (e) 4% of CNTs, and (f) average curves vs. percentage of CNTs. CNTs: carbon nanotubes.

SEM characterization of the delamination in tested specimens

Tested specimens were also analyzed using SEM. Figure 7 shows the surface morphology of the shear plane of the laminate tested under SBST. Generally, matrix cracks are observed, which are induced by the compressive stresses

under the loading zone. Inter and Intra-ply damage and fibers/matrix decohesion interface are also observed near the matrix cracks region. All microscopy images have shown that the delamination is the main failure modes observed in 0 and 90 directions for the shear test.

This microscopy characterization leads to the placement of the cohesive layers at the identified damage

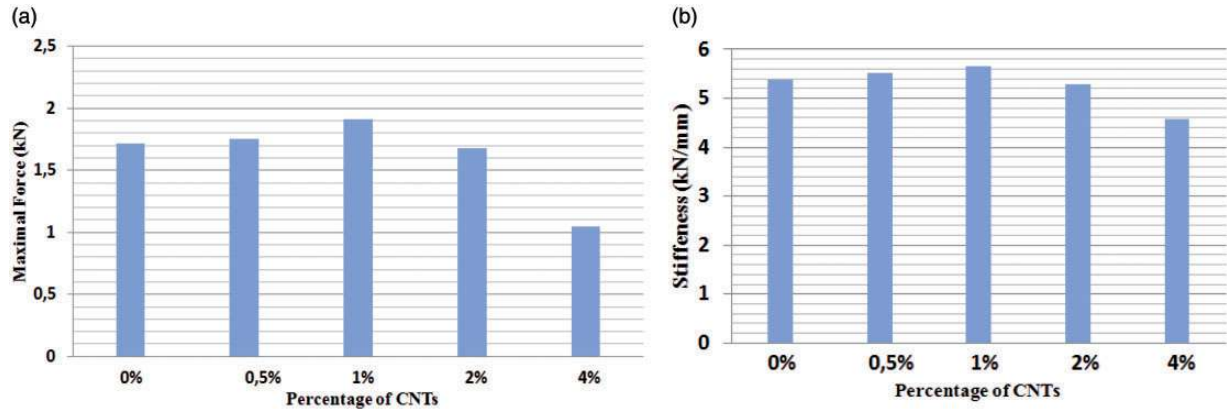


Figure 4. Mechanical properties of laminate vs. percentage of CNTs under shear test. (a) Force vs. percentage of CNTs, (b) Stiffness vs. percentage of CNTs.
CNTs: carbon nanotubes.

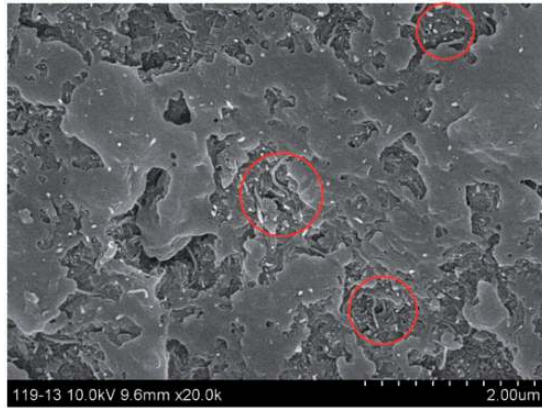


Figure 5. CNTs aggregate and the agglomeration of nanotubes creating cluster phase.
CNTs: carbon nanotubes.

zone in our numerical models. First, we were interested to investigate the delamination evolution. For that reason, the cohesive elements were considered and introduced in order to modeling the delamination and compared to the experimental results.

Damage modeling using CZM

Cohesive zone modeling technique was considered in various papers as a powerful tool to control the progressive delamination in composites under static tests¹¹ and for the dynamic impact.¹² In this section, CZMs were used to control multiple delaminations in the composite containing CNTs subjected to SBST. The interface elements considered in this study take the form of discrete elements between initially coincident nodes. Details of mathematical formulations and expression were given in open literature papers of the delamination modeling.^{13,14}

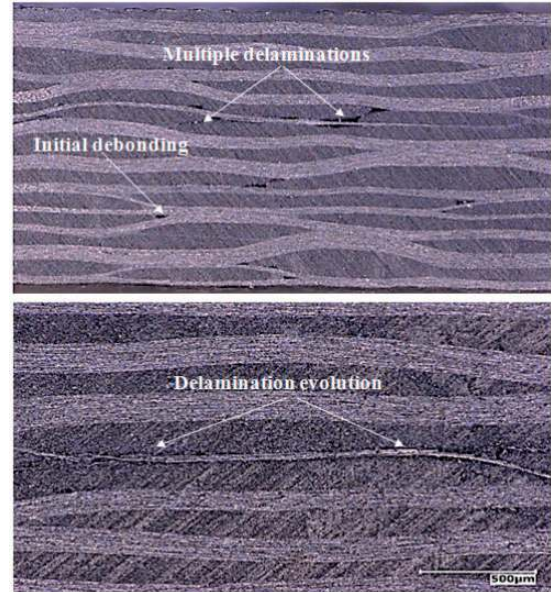


Figure 6. Keyence micrographs of specimens showing the delamination induced by SBST.
SBST: short beam shear test.

Establishment of the delamination

This section presents and recalls some formulations and criteria of the initiation and the evolution of delamination. According to Tarfaoui et al.,¹² when the interface is subject to pure I, or II loading modes, the delamination takes place if the inter laminar associated stress achieves its maximum interfacial value. Obviously, under mixed-mode loading, the delamination onset may occur before those maximum values are attained. The interaction between the stress components under

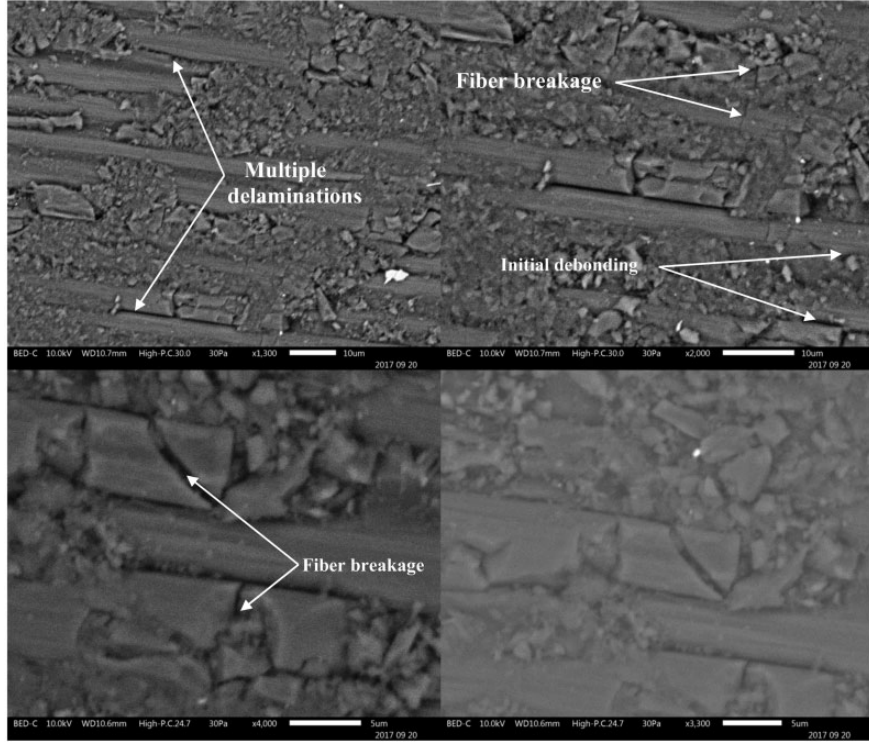


Figure 7. SEM images of tested specimens under SBST test.
SEM: scanning electron microscopy; SBST: short beam shear test.

Table I. Orthotropic elastic properties of component.¹⁵

	E_{11} (GPa)	$E_{22} = E_{33}$ (GPa)	G_{12} (GPa)	G_{13} (GPa)	G_{23} (GPa)	ν_{12}	ν_{13}	ν_{23}
Carbon fibers	230	15	15	15	15	0.2	0.2	0.2
Epoxy matrix	E (GPa)				ν			
CNTs	2.72				0.3			
	500				0.26			

CNTs: carbon nanotubes.

mixed-mode loading has to be taken into account by using a multi-axial stress criterion given by

$$\left(\frac{t_1}{t_1^0}\right)^2 + \left(\frac{t_2}{t_2^0}\right)^2 + \left(\frac{t_3}{t_3^0}\right)^2 = 1 \quad (1)$$

where t_1^0 , t_2^0 , and t_3^0 are the maximum inter laminar stress vector components along x_1 , x_2 , and x_3 directions, respectively.

Delamination propagates when the energy release rate attains its critical value under pure mode I, mode II or mode III fracture. The most widely used criterion to predict the propagation of the delamination under mixed-mode loading is the power law criterion initially

introduced in Jimenez¹⁴

$$\left(\frac{G_I}{G_{Ic}}\right)^n + \left(\frac{G_{II}}{G_{IIc}}\right)^n + \left(\frac{G_{III}}{G_{IIIc}}\right)^n = 1 \quad (2)$$

where n is an empirical parameter G_{Ic} , G_{IIc} , and G_{IIIc} are the critical energy release rates of the mode I, II, and III.

Material parameters and specimens

The sample was homogenized as an orthotropic elastic behavior. The mechanical properties and strength

parameters of Carbon fibers/Epoxy-CNTs composites used for the damage modeling were given in our previous works focuses on the homogenization of laminates composites based CNTs, see literature^{15–18} and listed in Tables 1 and 2, respectively.

Table 2. Homogenized orthotropic elastic properties of samples vs. CNTs fractions.¹⁵

	0%	0.5%	1%	2%	4%
E_{11} (GPa)	59.11	59.138	59.16	59.219	59.33
E_{22} (GPa)	59	59	59	59	58.55
E_{33} (GPa)	7.6	7.623	7.6	7.67	7.81
ν_{12}	0.089	0.089	0.0892	0.0892	0.0892
ν_{13}	0.27	0.27	0.27	0.274	0.275
ν_{23}	0.28	0.28	0.277	0.279	0.28
G_{12} (GPa)	8.250	8.257	8.270	8.285	8.316
G_{23} (GPa)	3.97	3.99	4.017	4.04	4.105
G_{13} (GPa)	0.27	0.27	0.27	0.274	0.275

CZM damage model discussed was used to describe the damage initiation and propagation in laminated composites with CNTs. The orthotropic elastic moduli and the strain energy release rate (modes I, II, and III) for CZM were given. There is no much works data for the fracture energies in the open literature for the case of CNTs; therefore, the values listed in Table 3 were proposed in Borowski et al.¹⁹ and used for numerical computations. The effect of CNTs on cohesive layer was observed and becomes important for the case of higher fractions.

Table 3. CZM properties.

	0%	0.5%	1%	2%	4%
G_{Ic} (kJ/m ²)	0.943	1.175	1.132	1.1	1.1
G_{IIc} (kJ/m ²)	0.1	0.1	0.1	0.1	0.1
G_{IIIc} (kJ/m ²)	0.1	0.1	0.1	0.1	0.1

CZM: cohesive zone model.

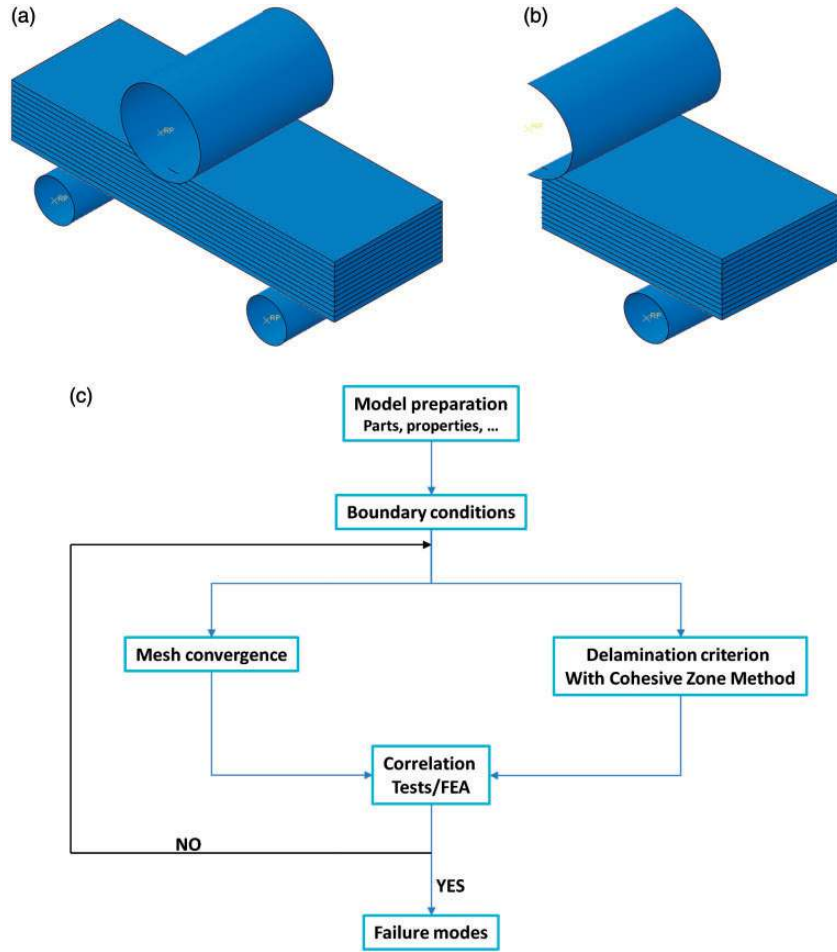


Figure 8. Finite element model of SBS test. (a) Full model, (b) $\frac{1}{2}$ model, and (c) follow chart of the numerical methodology. SBS: short beam shear.

Composite samples used in experimental tests are composed of Epoxy matrix bonded with CNTs and reinforced with 5HS carbon fibers fabric. SBST ASTM D2344 was considered to investigate on the damage initiation and delamination evolution. The geometry of specimens and the loading conditions are illustrated in Figure 8(a). Delamination modeling using CZM needs a large time and high memory space. Therefore, optimizing cost time computations and memory are considered, benefiting from the advantage of specimen symmetries. However, the only $\frac{1}{2}$ of the specimen dimensions can be used for simulations, with appropriate symmetry as shown in Figure 8(b). The follow chart of the numerical methodology is presented in Figure 8(c).

Implementation of cohesive elements

The symmetry of the composite specimens was considered in order to optimize time and memory computations. The cohesive interface element was embedded into specimens. Figure 9 shows a typical SBST model with solid elements and the zone where interface elements are inserted. Cohesive elements were implanted between each ply surface in order to predict the delamination. Also at locations within each ply, lines of elements were inserted to model the intra-ply splitting and matrix cracking.

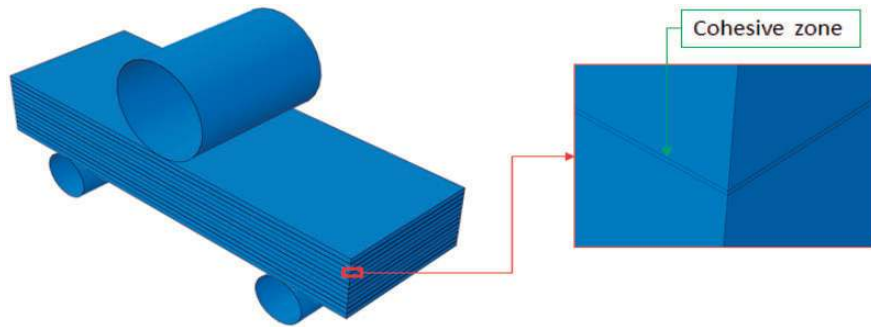


Figure 9. Model and locations where interface elements were inserted.

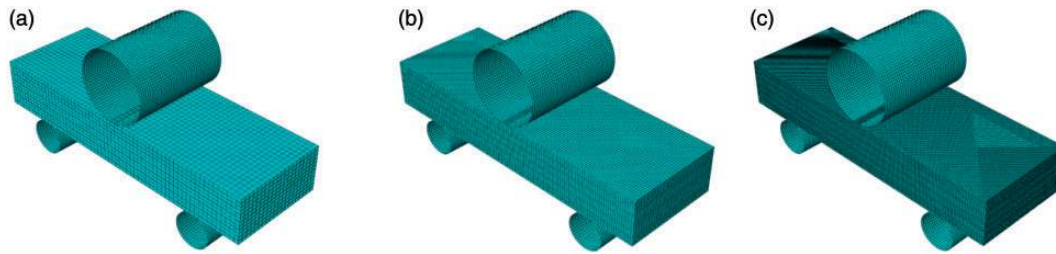


Figure 10. Example of mesh resolutions used for convergence study. (a) Mesh size = 0.4 mm, (b) mesh size = 0.2 mm, and (c) mesh size = 0.1 mm.

Meshes and mesh convergence

The mesh convergence is firstly studied in order to determine the minimum number of elements for which the convergence was started²⁰⁻²³ and then the damage can be predicted. For that purpose, different mesh resolutions were tested and presented in Figure 10. Figure 11 presents the variation of the maximum Von Mises stress vs. the number of elements under SBST. This figure shows that a mesh density of 20,000 elements can provide a good prediction of the damage evolution.

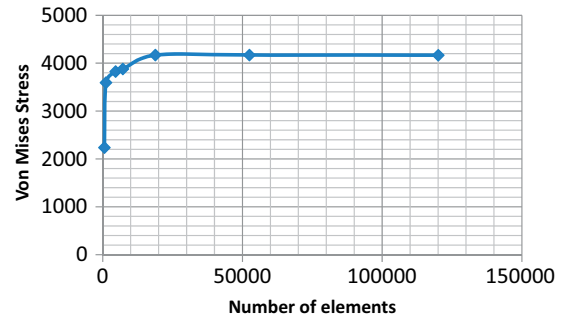


Figure 11. Mesh convergence: maximum Von Mises stress vs. number of elements.

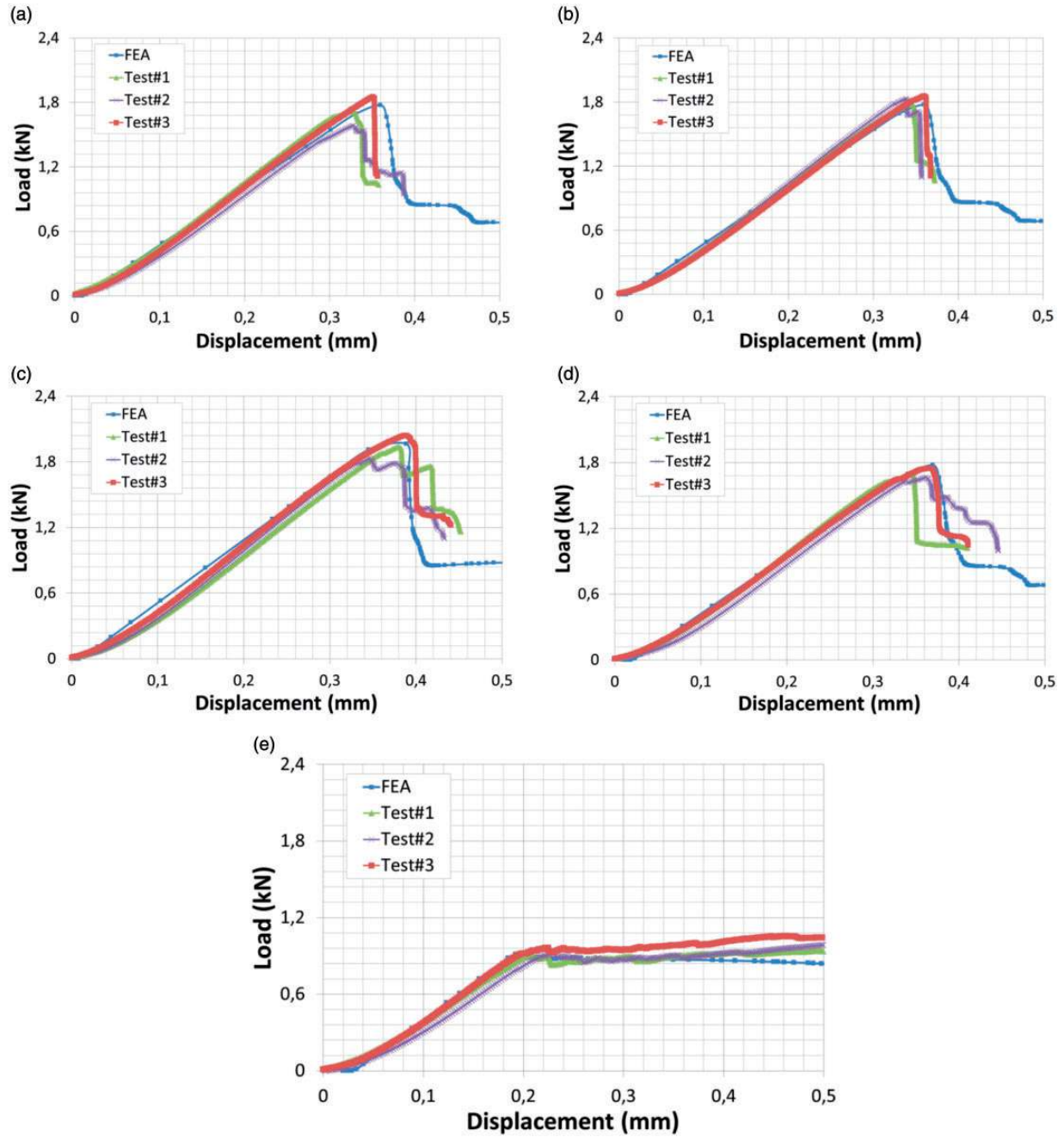


Figure 12 : SBST—CZM: confrontation of experimental data and numerical results for different CNTs fractions. (a) 0% of CNTs, (b) 0.5% of CNTs, (c) 1% of CNTs, (d) 2% of CNTs, and (e) 4% of CNTs.

SBST: short beam shear test; CZM: cohesive zone model; CNTs: carbon nanotubes.

Confrontation of numerical results and experimental data

The numerical load–displacement curves obtained using cohesive elements for different CNTs fractions are shown in Figure 12 and compared with experimental curves. These results show a good tendency between numerical variation and experimental data. Similar to experimental variation, the numerical response based

CZM shows three distinct regions: initial elastic region, a maximum load and the net fracture. Numerical results follow closely experimental data even damaged part. From numerical and experimental results, the adding of a minor amount of CNTs improves shear resistance of laminates, but with high CNTs fractions, the resistance of composites is decreased.

The numerical computations on nanotubes filled laminate based shear tests provides also access to local

properties. A contour plot of the Mises stress concentration is presented and analyzed. Figure 13 illustrates a map of the stress concentration vs. CNTs fraction. A heterogeneous distribution of stress is observed within specimens for different CNTs fraction. The concentration is observed in three principal zones namely; under indenter and around of the support points and the delamination initiates and propagates at similar regions, i.e. at the zone of stress concentration.

The contour plot shows high stress concentration for the case of 0%-CNTs and decreases progressively with increasing CNTs fraction. The maximum of stress changes with changing the CNTs fractions, which means that the nanotubes affect the initiation of damage and the delamination of laminate panels. Maximum values of the stress concentration are obtained in the case of 0% of CNTs and decrease by adding the CNTs. For that, CNTs tend to improve the

interfacial resistance and retard the damage initiation and the delamination evolution.^{24,25}

Delamination in the numerical model vs. CNTs concentration

Numerical loading was applied using a prescribed displacement on the nodes placed under indenter. Nodes above supports were fixed. Loads are applied perpendicular to the top surface. Eventually, increasing loading starts to induce the specimen damage and delamination between plies.

Figure 14 shows the progressive damage accumulation and delamination evolution in specimens under SBST for different tested panels. Initially, at small load damage accumulates under indenter and points support without cracking. As the load increases, a delamination crack appears and propagates in the form of axial cracks.

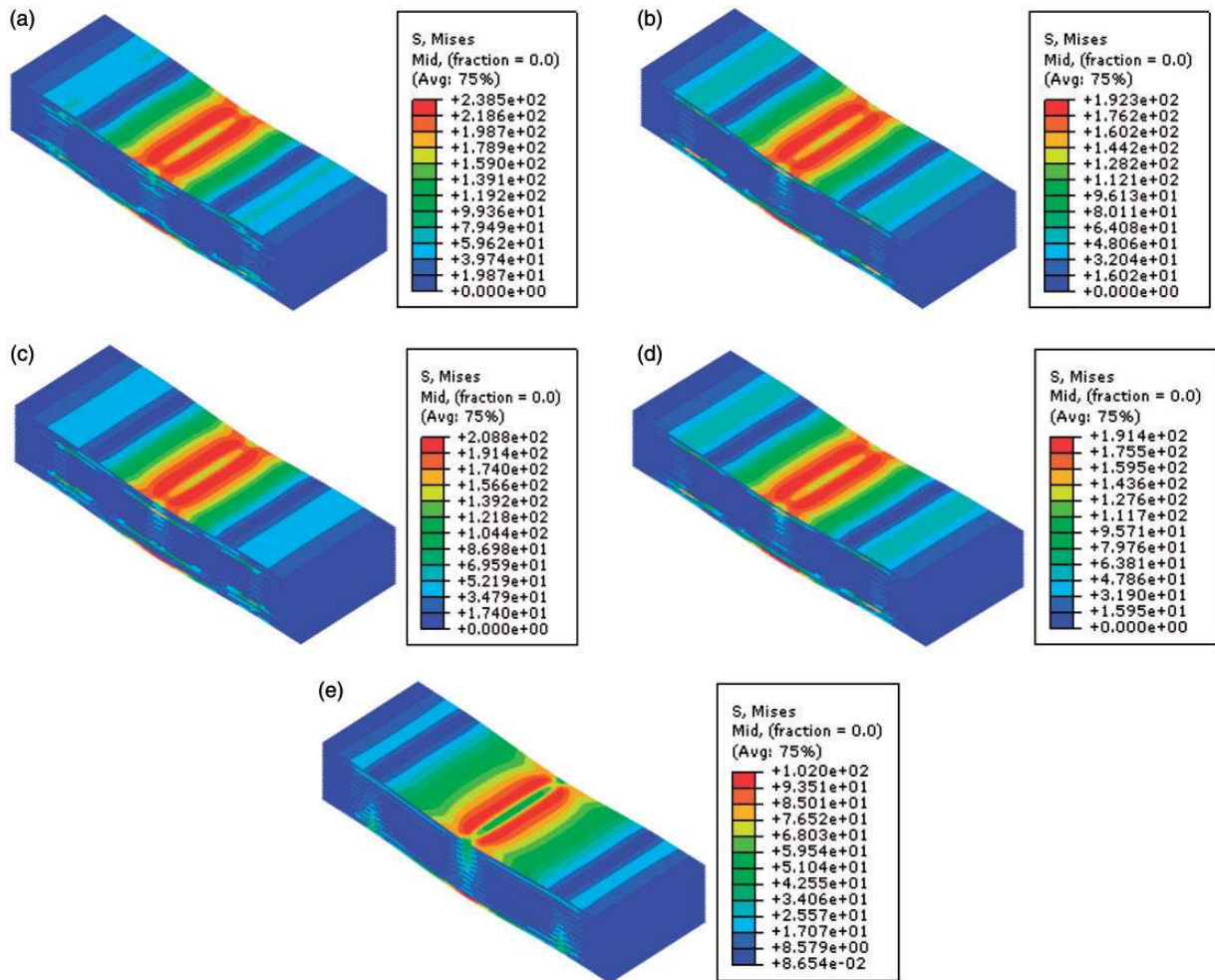


Figure 13. Stress concentration under SBST for specimens with and without CNTs. (a) 0% of CNTs, (b) 0.5% of CNTs, (c) 1% of CNTs, (d) 2% of CNTs, and (e) 4% of CNTs.

SBST: short beam shear test; CNTs: carbon nanotubes.

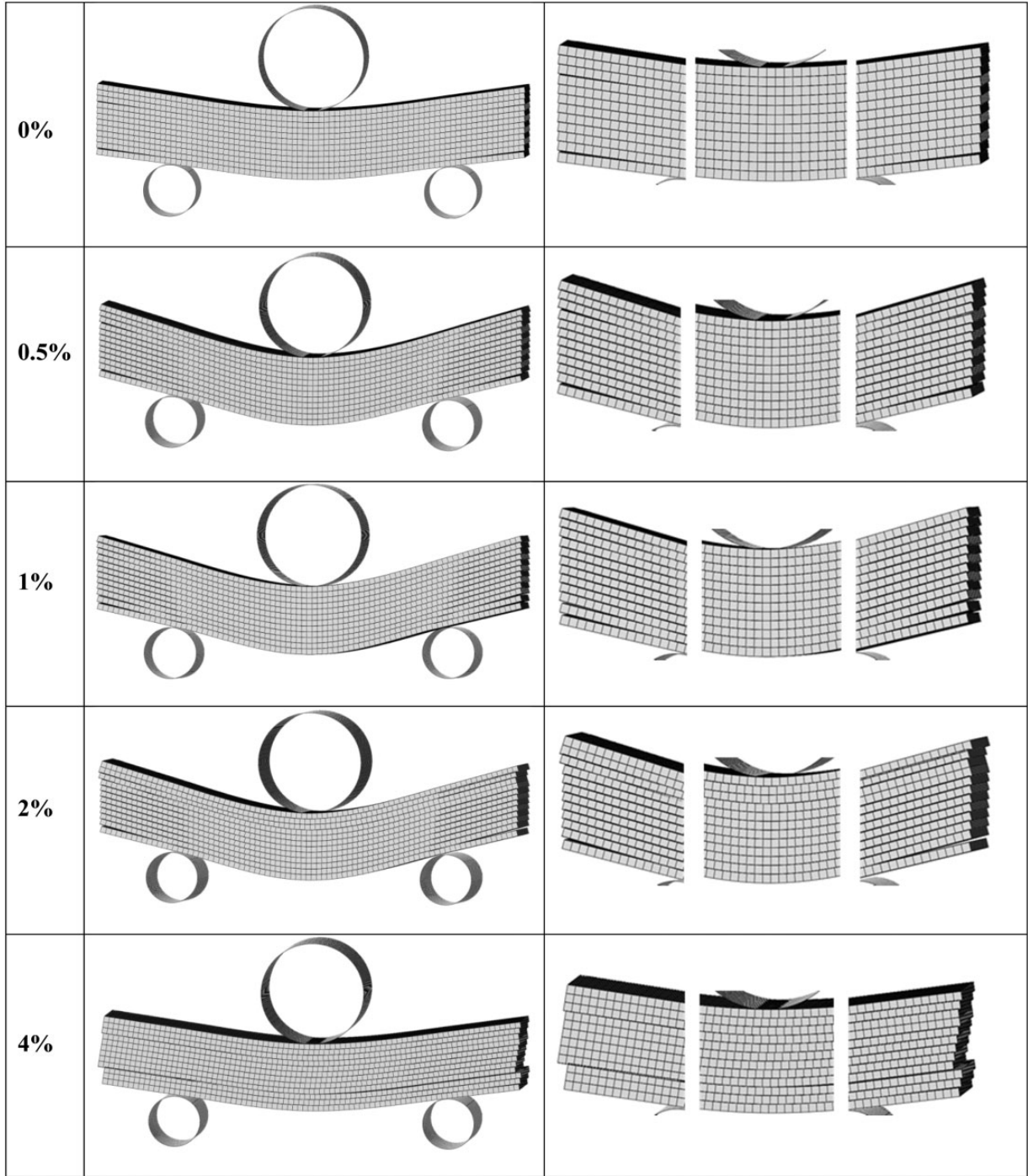


Figure 14. Visualization of predicted delamination vs. CNTs in laminated composites.
CNTs: carbon nanotubes.

Therefore, the delamination develops in the cohesive zone along the longitudinal direction of specimens. The observed delamination in the case of 0%-CNTs is differed to that one of 4%-CNTs. Addition of minor amounts of CNTs enhances the interfacial resistance of composites,²⁶ but with high CNTs fractions, the resistance decreases and the delamination becomes important.

Conclusion

In this paper, the experimental characterization was first performed to investigate the delamination evolution in laminate composites reinforced with CNTs. The specimens were tested under SBST at various CNTs fractions. Microscopy analysis of tested samples showed that the

matrix cracking, Intra and Inter delamination were the dominant damage modes at the specimens. These micro-structural characterizations formed a basis for damage incorporation and lead to implantation of the cohesive element in the developed numerical models.

The results of numerical models were in good agreement compared to the experimental data. Numerical models were developed and have produced the same delamination observed experimentally. The effect of CNTs was studied. It appeared that a small amount of CNTs used additives had enhanced the interfacial resistance and causes a delay in the delamination. However with higher CNTs fractions (about 4%), the resistance had decreased, and the delamination evolution became important. The top and the bottom layers of the laminate specimens experienced delamination failure at different CNTs fractions, whereas the delamination appears at central layers in the case of 4% of CNTs. Therefore, using higher amounts of CNTs in laminate composites had decreased the rigidity and fracture toughness and also can promote the delamination evolution.


Declaration of Conflicting Interests

The author(s) declared no potential conflicts of interest with respect to the research, authorship, and/or publication of this article.

Funding

The author(s) disclosed receipt of the following financial support for the research, authorship, and/or publication of this article: This work was funded by DGA (Direction Générale de l'Armement (DGA—Ministry of Defense), MRIS project: Study of composites reinforced with carbon nanotubes (CNT). The Authors of this paper gratefully acknowledge the financial support of the DGA, France.

ORCID iD

A El Moumen  <http://orcid.org/0000-0002-3291-8532>

References

1. Hamitouche L, Tarfaoui M and Vautrin A. An interface debonding law subject to viscous regularization for avoiding instability: application to the delamination problems. *Eng Fracture Mech* 2008; 75: 3084–3100.
2. Camanho PP, Davila CG and De Moura MF. Numerical simulation of mixed-mode progressive delamination in composite materials. *J Compos Mater* 2003; 37: 1415–1424.
3. Li T, Mo J, Yu X, et al. Mechanical behavior of C/SiC composites under hypervelocity impact at different temperatures: micro-structures, damage and mechanisms. *Compos Part A Appl Sci Manuf* 2016; 88: 19–26.
4. Ullah H, Harland AR and Silberschmidt VV. Experimental and numerical analysis of damage in woven GFRP composites under large-deflection bending. *Appl Compos Mater* 2012; 19: 769–783.
5. Arbaoui J, Tarfaoui M and El Malki Alaoui A. Mechanical behavior and damage kinetics of woven E-glass/vinylester laminate composites under high strain rate dynamic compressive loading: Experimental and numerical investigation. *Int J Impact Eng* 2016; 87: 44–54.
6. Lachaud F, Espinosa C, Michel L, et al. Modelling strategies for simulating delamination and matrix cracking in composite laminates. *Appl Compos Mater* 2015; 22: 377–403.
7. Lachaud F, Espinosa C, Michel L, et al. Modelling strategies for predicting the residual strength of impacted composite aircraft fuselages. *Appl Compos Mater* 2015; 22: 599–621.
8. Jacques S, De Baere I and Van Paepegem W. Analysis of the numerical and geometrical parameters influencing the simulation of mode I and mode II delamination growth in unidirectional and textile composites. *Appl Compos Mater* 2015; 22: 637–668.
9. Kumar D, Roy R, Kweon JH, et al. Numerical modeling of combined matrix cracking and delamination in composite laminates using cohesive elements. *Appl Compos Mater* 2016; 23: 397–419.
10. Coelho AMG. Finite element guidelines for simulation of delamination dominated failures in composite materials validated by case studies. *Arch Comput Methods Eng* 2016; 23: 363–388.
11. Yousefi J, Mohamadi R, Saeedifar M, et al. Delamination characterization in composite laminates using acoustic emission features, micro visualization and finite element modeling. *J Compos Mater* 1–13. DOI: 10.1177/0021998315615691.
12. Tarfaoui M, Gning PB and Hamitouche L. Dynamic response and damage modelling of glass/epoxy tubular structures: numerical investigation. *Compos Part A Appl Sci Manuf* 2008; 39: 1–12.
13. Riccio A and Gigliotti M. A novel numerical delamination growth initiation approach for the preliminary design of damage tolerant composite structures. *J Compos Mater* 2007; 41.
14. Jimenez MA. Application of the finite-element method to predict the onset of delamination growth. *J Compos Mater* 2004; 38.
15. El Moumen A, Tarfaoui M and Lafdi K. Computational homogenization of mechanical properties for laminated composites reinforced with thin film made of carbon nanotubes. *Appl Compos Mater* Epub ahead of print 18 August 2017. DOI: 10.1007/s10443-017-9636-2.
16. Tarfaoui M, Lafdi K and El Moumen A. Mechanical properties of carbon nanotubes based polymer composites. *Compos Part B Eng* 2016; 103: 113–121.
17. Tarfaoui M, El Moumen A and Lafdi K. Progressive damage modeling in carbon fibers/carbon nanotubes reinforced polymer composites. *Compos Part B Eng* 2017; 112: 185–195.
18. El Moumen A, Tarfaoui M and Lafdi K. Mechanical characterization of carbon nanotubes based polymer composites using indentation tests. *Compos Part B Eng* 2017; 114: 1–7.

19. Borowski E, Soliman E, Kandil UF, et al. Interlaminar fracture toughness of CFRP laminates incorporating multi-walled carbon nanotubes. *Polymers* 2015; 7: 1020–1045.
20. El Moumen A, Kanit T, Imad A, et al. Effect of reinforcement shape on physical properties and representative volume element of particles-reinforced composites: statistical and numerical approaches. *Mech Mater* 2015; 83: 1–16.
21. Kaddouri W, El Moumen A, Kanit T, et al. On the effect of inclusion shape on effective thermal conductivity of heterogeneous materials. *Mech Mater* 2016; 92: 28–41.
22. Bouaoune L, Brunet Y, El Moumen A, et al. Random versus periodic microstructures for elasticity of fibers reinforced composites. *Compos Part B Eng* 2016; 103: 68–73.
23. Beicha D, Kanit T, Brunet B, et al. Effective transverse elastic properties of unidirectional fiber reinforced composites. *Mech Mater* 2016; 102: 47–53.
24. El Moumen A, Tarfaoui M, Lafdi K, et al. Dynamic properties of carbon nanotubes reinforced carbon fibers/epoxy textile composites under low velocity impact. *Compos Part B Eng* 2017; 125: 1–8.
25. El Moumen A, Tarfaoui M, Hassoon O, et al. Experimental study and numerical modelling of low velocity impact on laminated composite reinforced with thin film made of carbon nanotubes. *Appl Compos Mater*. DOI: 10.1007/s10443-017-9622-8.
26. Benyahia H, Tarfaoui M, Datsyuk V, et al. Dynamic properties of hybrid composite structures based multi-walled carbon nanotubes. *Compos Sci Technol* 2017; 148: 70–79.